10.1515/astro-2017-0124

Baltic Astronomy, vol. 25, 225–235, 2016

DEPRESSED EMISSION BETWEEN MAGNETIC ARCADES NEAR A SUNSPOT

B. I. Ryabov[1] and K. Shibasaki[2]

[1] *Ventspils International Radio Astronomy Center, Inzhenieru str. 101a, Ventspils, LV-3601, Latvia; ryabov@latnet.lv*

[2] *Solar Physics Research Inc., Matsushin 2-24, Kasugai 486-0931, Japan; shibasaki.kiyoto@md.ccnw.ne.jp*

Received: 2016 February 15; accepted: 2016 April 21

Abstract. The locations of the depressed emission in microwaves, EUV and soft X-rays are compared with each other and with the location of the plasma outflow in the active region (AR) 8535 on the Sun. We found that two open-field regions overlap the regions of depressed emission near the AR's sunspot. These two open-field regions are simulated with the potential-field source-surface (PFSS) model under radial distances of $R_{\rm SS} = 1.8\ R_\odot$ and $R_{\rm SS} = 2.5\ R_\odot$. Each open-field region is located between the arcades of the loops of the same magnetic polarity. The former open-field region covers the region of the plasma outflow, which is thus useful for the tests on connection to the heliosphere. The utmost microwave depression of the intensity in the ordinary mode (the Very Large Array 15 GHz observations) also overlaps the region of the plasma outflow and thus indicates this outflow. The lasting for eight days depression in soft X-rays and the SOHO EIT $2.84{\times}10^{-8}$ m images are attributed to the evacuation of as hot coronal plasma as $T \geq 2 \times 10^6$ K from the extended in height ("open") magnetic structures. We conclude that the AR 8535 presents the sunspot atmosphere affected by the large-scale magnetic fields.

Key words: Sun: sunspots, radio radiation, EUV, X-rays, magnetic fields

1. INTRODUCTION

Some bipolar active regions (ARs) have proven to be the sources of plasma outflows in the narrow band of different magnetic connectivity at the borders of the ARs (Del Zanna 2008; Baker et al. 2009; Mandrini et al. 2015). Such bands are observed as the regions of depressed coronal emission and characterized by low coronal plasma density and unipolar magnetic field (Doschek et al. 2008). They persist for days at the same locations in ARs. Some more observational features have proven to be well-elaborated tools for the investigation on the plasma outflow in the bipolar ARs. Unlike the bipolar ARs, the isolated sunspots are not sufficiently investigated.

The notion of the dark band was first introduced by Švestka et al. (1977) as "dark coronal corridor", but subsequently became "dark band" since it appears dark under a wide range of temperatures (Scott, Martens & Tarr 2013). The term

"coronal parting" (CP) is used by Nikulin & Dumin (2016) on the global scale of the Sun. The simulated magnetic structure of the CP shows the band of open field lines separating two magnetic arcades. The closest to the band photospheric footpoints of the loops are of *the same magnetic polarity* but directed oppositely with strong divergence. This magnetic structure looks like the partition of two parts in a person's hairs.

Nikulin & Dumin (2016) stated that the CP with a different X-ray brightness at the opposite sides occurs in the case of the different gradients of magnetic field: the higher the gradient, the higher the brightness of coronal emission. CP might pass through an isolated sunspot and a set of CPs might separate a bipolar AR. The authors noted that CP is associated with the region of a few percent brighter than the background in the chromospheric absorption line He 1.083 μm. In the lower layers of the atmosphere the CP is associated with the parallel rows of unipolar magnetic knots.

In this work, we compare the location of the sampled and earlier published observational features with the location of the plasma outflow in the large sunspot of the AR 8535 (Brosius & Landi 2005). The cool loop fans (CLFs) clearly seen in the Transition Region and Coronal Explorer (TRACE) 1.71 $\times 10^{-8}$ m images, as well as the CPs, and the regions of reduced microwave emission are tested as indicators of the plasma outflows and magnetic peculiarities. CLF can indicate the region of the plasma outflow (Warren et al. 2011) and the separation of the domains of coronal loops (Schrijver et al. 2010).

To analyze the observed CPs and the involvement of the sunspot fields into the global magnetic structures we make use of the PFSS model, where the entire field lines at the radial distances $r > R_{\rm SS}$ are taken as open (Altschuler & Newkirk 1969; Schatten et al. 1969). If one proves the real "openness" of the field lines and the connection to the heliosphere, he/she should undertake a set of special investigations (Slemzin et al. 2013), which are out of the scope of this work.

The reduced microwave emission was analyzed by Ryabov et al. (2015) as the counterpart of the depressed coronal emission in the periphery of the large isolated sunspots. This work continues to trace an analogy between the occurrence of the depressed emission, including microwave depression, in isolated sunspots and bipolar ARs. We make use of the Nobeyama Radioheliograph (NoRH) 17 GHz observations and the Very Large Array (VLA) microwave observations published by Brosius & White (2004) and Loukitcheva, Solanki & White (2014).

2. OBSERVATIONS AND PFSS SIMULATIONS

2.1. Microwave observations

2.1.1. VLA observations

Brosius & White (2004) obtained the coordinated EUV and radio observations of the large sunspot NOAA 8535 with the Solar and Heliospheric Observatory (SOHO) instruments (CDS, EIT, MDI) and the VLA on 1999 May 9 and 13. The spatial resolution of the VLA was about $15''$, $10''$, and $5''$ at frequencies of 5 GHz, 8 GHz, and 15 GHz, respectively. It is necessary to note here that this publication cites the involved AR 8535 as the AR 8539.

The authors attributed the total intensity (Stokes I) peaks to the gyro-resonance

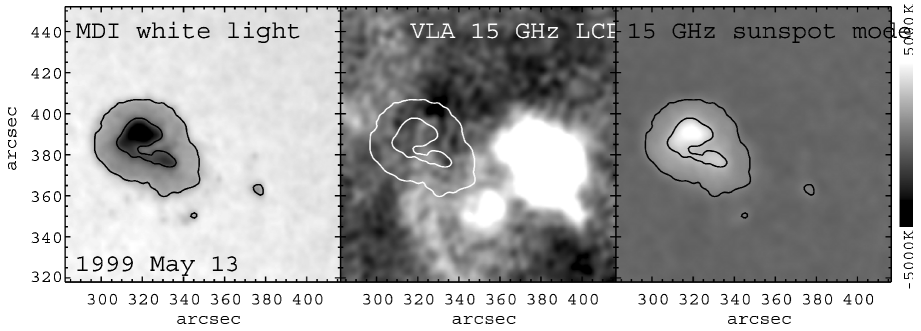

Fig. 1. The large sunspot in the AR 8535 on 1999 May 13: the SOHO MDI white light image (left panel); the VLA image of the intensity in left-hand circular polarization (o-mode in this case of positive magnetic polarity) at 15 GHz (middle panel); the image recalculated from the white light image (right panel). The brightness temperature range at 15 GHz is from –5000 to 5000 K relative to the quiet Sun level. This figure adopted from Loukitcheva, Solanki & White (2014) and reproduced with permission from Astronomy and Astrophysics, © ESO.

sources from the sunspot plumes seen in the EUV emission lines formed at $T = (1.6 - 5) \times 10^5$ K. The microwave depression is clearly seen in Stokes I and V at 5 GHz and 8 GHz (panels 4c and 4f in Brosius & White 2004) when the sunspot was located at N20°, W21° on May 13. No microwave depression was reported at the sunspot location N22°, E30° on May 9.

Loukitcheva, Solanki & White (2014) presented the VLA observations of the AR 8535 at 15 GHz in the magnetoionic ordinary (o-) mode (Fig. 1) to eliminate the bright gyro-resonance radiation dominating in the extraordinary (x-) mode. They concluded that existing models of the sunspot atmosphere predict a bright core of 15 GHz source in the o-mode that contradicts the near-background level of the intensity observed with the VLA in the core of this sunspot-associated source (Fig. 1).

Let us note that the region of the utmost depression of 15 GHz emission in o-mode at the northern border of the sunspot overlaps the region of the negative Doppler velocities in a set of the EUV emission lines observed with the SOHO CDS by Brosius & Landi (2005) (see Fig. 3e in their publication).

Iwai et al. (2016) confirmed that the umbra of relatively large and isolated sunspots provides the brightness temperature of the emission in long millimeter range (in Stokes I at 34 GHz) much lower than predict the current models of the sunspot atmosphere. Again, it is about the same as the brightness temperature of the surrounding quiet region.

2.1.2. NoRH observations

The Nobeyama Radioheliograph (NoRH) provides Stokes V and I maps of the Sun at 17 GHz with an angular resolution of 18″. Here we synthesize and clean the maps in right (R) and left (L) circular polarization using a set of the identical parameters.

The predominance of the radiation in magnetoionic x-mode over o-mode in a stable sunspot-associated source is well established. Hence, in the case of the x-mode radiation, the one-to-one correspondence holds for R(L) circular polarization

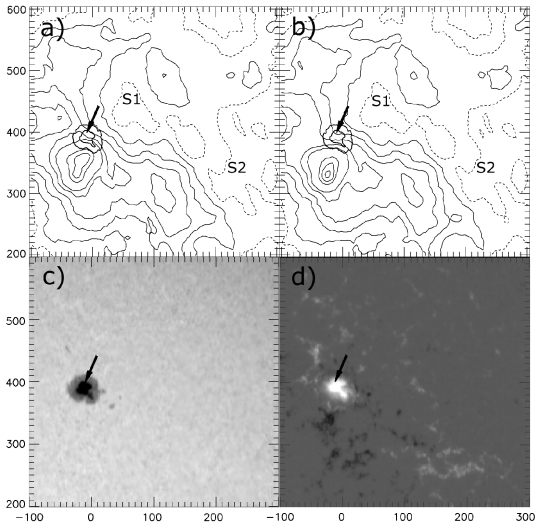

Fig. 2. 1999 May 12 observations of the large sunspot in the AR 8535: (a) the brightness temperature $T_{\rm x}^{\rm B}$ and (b) $T_{\rm o}^{\rm B}$ contour maps of 17 GHz images (NoRH). Here and in the panels 3a and 3b the levels of $T_{\rm x}^{\rm B}$ and $T_{\rm o}^{\rm B}$ are at 0.9, 1.0 (dashed line) and 1.1, 1.2, 1.3, 1.4, 1.5, 2.0, 2.25, 2.5 (solid line) in units of 10^4 K. The arrow points to the location of the reduced emission in o-mode. (c) The white light image (NSO/KP) and (d) the longitudinal magnetogram (SOHO MDI). The axis units are in seconds of arc from the center of the solar disk; solar north is up, solar west is to the right.

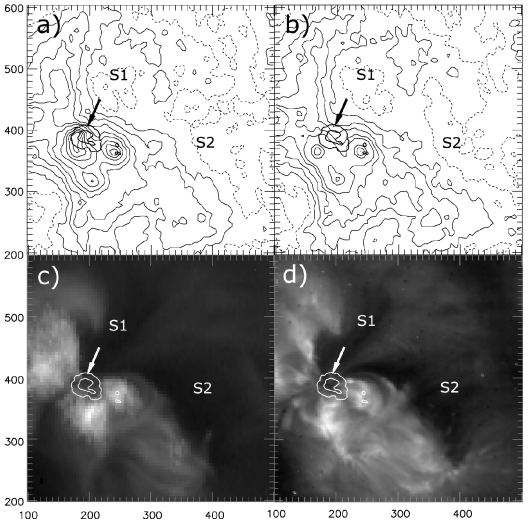

Fig. 3. 1999 May 13 observations of the large sunspot in the AR 8535: (a) the brightness temperature $T_{\rm x}^{\rm B}$, and (b) $T_{\rm o}^{\rm B}$ contour maps of 17 GHz images (NoRH); (c) the soft X-ray image (Yohkoh/SXT), and (d) the EUV 2.84 $\times 10^{-8}$ m image (SOHO EIT).

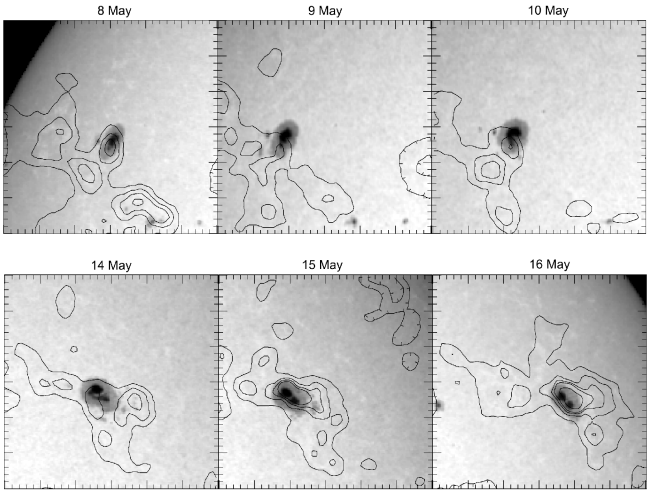

Fig. 4. Total intensity (Stokes I) contour maps of 17 GHz images (NoRH) overlaid on white-light images (SOHO MDI continuum). The brightness temperature $T_{\rm I}^{\rm B}$ levels are as follows: 0.9, 1 (downhill line), 1.5, 2, 2.5, 3, and 5 (solid line) in units of 10^4 K.

and the N(S) magnetic fields of the sunspot; and vice versa in the case of the o-mode radiation.

Figures 2 and 3 compare the 17 GHz contour maps in the x-mode and o-mode with the photospheric and coronal images. The arrow points to the concave contour of the o-mode emission, which signals the local microwave depression. The depression in o-mode of 2% (Fig. 2b) overlaps the utmost microwave depression at 15 GHz (middle panel of Fig. 1) at the northern border of the sunspot umbra. Note that the 17 GHz depression detected on May 13 (Fig. 3b) is less pronounced. The reduced 17 GHz emission as the counterparts of the large-scale dark coronal structures S1 and S1 are noticeable outside the sunspot on both dates of May 12 and 13.

Figure 4 shows that the round bright core of 17 GHz sunspot-associated source is absent while the sunspot is near the central meridian passage (CMP). The round core formed by contours in the range $\rm T_I^B = (3–8)\times10^4$ K appears near the solar limbs on May 15–18 and May 7–8, that is, within the moderate distances from the central solar meridian. It bears evidence of transparent gyro-resonance layers at 17 GHz while near the CMP. As for 15 GHz gyro-resonance radiation, Brosius & White (2004) noted only a compact source of the size less than the sunspot umbra on May 9 and May 13.

2.2. Coronal structures

The dark large-scale coronal structures S1 and S2 are clearly seen in the SOHO EIT 2.84×10^{-8} m and Yohkoh/SXT images from May 8 until May 15, but hardly distinguishable at lower formation temperatures in the EIT 1.71×10^{-8} m and 1.95×10^{-8} m images (Fig. 5).

Harrison et al. (2003) argued that the eruption of prominence and the coronal mass ejection (CME) on the east solar limb on May 8 was accompanied by the

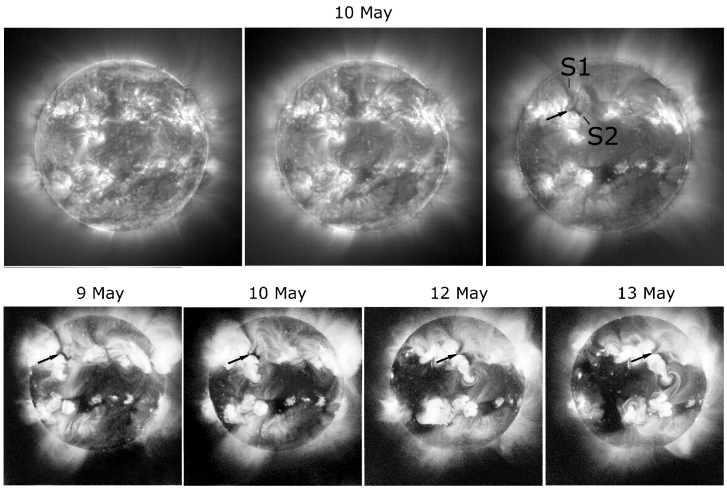

Fig. 5. EUV images in the 1.71×10^{-8} m, 1.95×10^{-8} m, and 2.84×10^{-8} m (from left to right in upper row) obtained with the SOHO EIT, and soft X-ray images obtained with the Yohkoh/SXT (lower row). The dark coronal structures S1 and S2 extend from the AR 8535 (arrow points to the site of the sunspot).

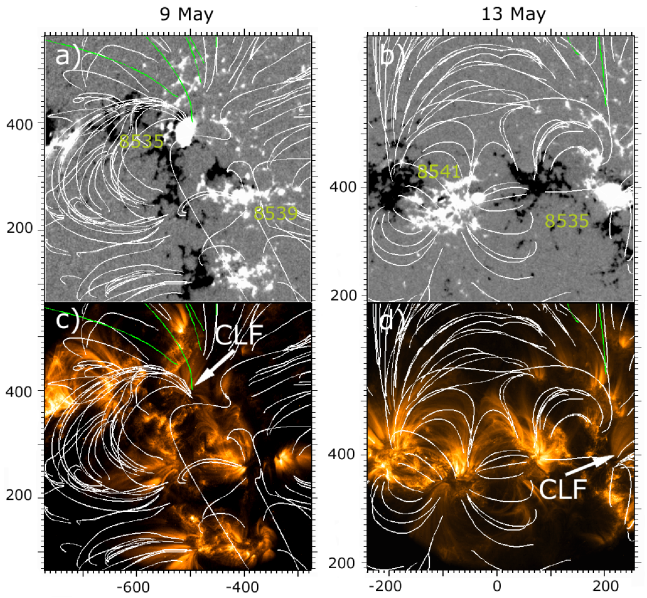

Fig. 6. Magnetic field lines extrapolated with the PFSS model and overlaid on the SOHO MDI magnetograms in panels (a) and (b). The background of panels (c) and (d) are the TRACE 1.71×10^{-8} m EUV images. (Courtesy of the Lockheed Martin Solar and Astrophysics Laboratory.)

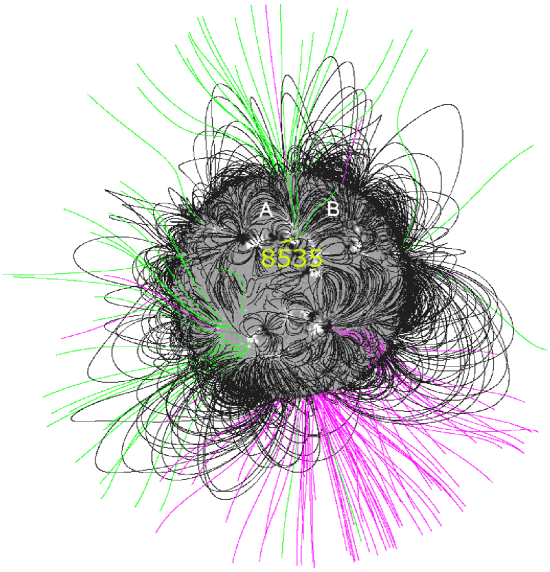

Fig. 7. Magnetic field lines of the "haired" Sun for the Carrington rotation number 1949 calculated with the PFSS model under $R_{SS} = 2.5\ R_{\odot}$. The open field lines to the north of the sunspot 8535 (green color) parting the photospheric footpoints of the strongly diverging loops of the same magnetic polarity in two arcades, "A" and "B" (field lines of black color). This open-field region is further denoted as the CP1.

mass loss in the low corona. Another start time for the dark structures S1 and S2 can be the CME overlying the ARs 8541 and 8535 on May 7 (Suzuki, Sakurai & Ichimoto 2006). We cannot resolve the origin of S1 and S2 with confidence since these structures are not distinguishable on May 7 but become darkest on May 9. However, we suggest the long-lasting deficit of high-temperature plasma, $T > 2 \times 10^6$ K, in these dark structures, since the formation temperature of the Fe XV emission line is about $2{\times}10^6$ K for the SOHO EIT $2.84{\times}10^{-8}$ m images (Moses et al. 1997).

According to the results of the next section (§2.3), the dark coronal structures S1 and S2 are the CPs. Each CP consists of two bright arcades of loops and a dark extended structure in between. In the case of the AR 8535, the X-ray brightness of the eastern arcade is higher than the western one (Fig. 5).

Figure 6 shows the small-scale structures observed as the fans of cool loops in the images taken in the TRACE $1.71{\times}10^{-8}$ m channel. These EUV images, which are sensitive to the emission at $T \leq 10^6$ K, show the CLFs emanating from the vicinity of the sunspot. The CLF of interest (pointed to by white arrow) is rooted near the region of the maximum Doppler upward velocity measured by Brosius & Landi (2005) and the region of the utmost 15 GHz depression in o-mode in Fig. 1.

2.3. PFSS simulations of field lines

The PFSS model is chosen to compute the field lines between the $r = R_{\odot}$ level, where the radial magnetic field distribution is specified, and the source surface level $r = R_{SS}$, where the field vector is taken to be radial with intension to simulate the solar wind outflow. The only free model parameter is the radial distance R_{SS}.

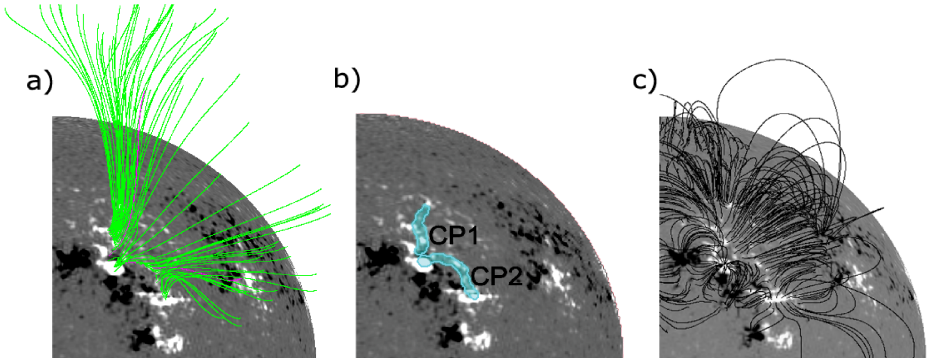

Fig. 8. The results of the PFSS model simulations overlaid on the full-sphere SOHO MDI magnetograms: (a) open magnetic field lines, (b) contours comprising two open-field regions, and (c) closed magnetic field lines of the magnetic arcades. The model parameter $R_{SS} = 1.8\ R_{\odot}$ is adjusted to reveal the open field lines of the coronal parting CP2. Note the rows of the magnetic knots of positive polarity (white color) inside the open-field regions in panel 8b.

The PFSS model allows tracing the extended ("open") field lines. The accuracy of PFSS modeling equals the resolution of the MDI input magnetic field, that is, 0.5 of heliographic degree (Schrijver, DeRosa & Title 2010). The field lines are extrapolated from the full-sphere SOHO MDI magnetograms (Fig. 7) using the SolarSoft routines (Schrijver & DeRosa 2003).

The PFSS simulations of the global coronal field lines under $R_{SS} = 2.5\ R_{\odot}$ (Schrijver & DeRosa 2003) present the AR 8535 as well. A chain of the patches of the open-field regions extends from the sunspot 8535 to the northeast direction up to the polar coronal hole. These patches persist all the time during the Carrington rotation number 1949 and represent a global coronal parting.

A new open-field region is revealed by diminishing the free parameter down to $R_{SS} = 1.8\ R_{\odot}$ in between the ARs 8535 and 8539. Note that the photospheric footpoints of the open field lines CP2 (Fig. 8b) resemble the observed dark coronal structure S2 (panel 3d). We have proved that the form of the darkest part of S2 nearly corresponds to the form of the open-field region CP2 in the course of solar axis rotation, as if S2 locates deep in coronal layers.

3. DISCUSSION AND CONCLUSIONS

In Fig. 9 we compile the above discussed features to resume the comparison of the observational features indicating the peculiarities of magnetic and emission structures.

We find that CP is useful as the observational feature indicating open-field region. The CPs in the bipolar ARs tend to cross nearly perpendicular the axis between the sunspots of opposite polarity (Nikulin & Dumin 2016). Near the large sunspot in the AR8535 the direction of the CP1 seems to be more dependent on the large-scale fields in the sense that the involved magnetic arcades originate on the large scale from the AR to the northern polar region (Schrijver & DeRosa 2003).

Instead of observed CP, one can use the computations of quasi-separatrix layers (QSLs) in the case of the rigorous topological presentation of the field line connec-

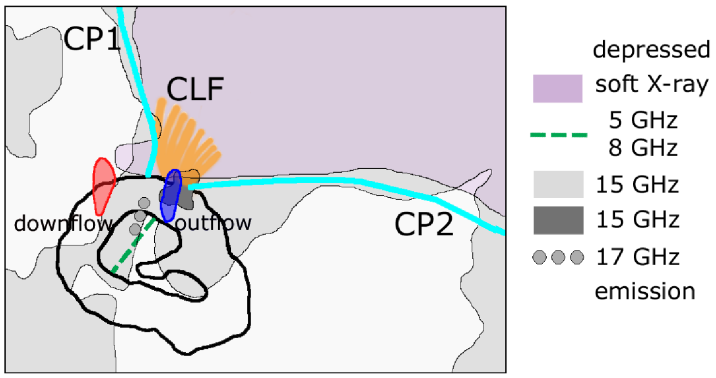

Fig. 9. The schematic picture of the observational features (depressed emission and cool loop fan) indicating the peculiarities (plasma outflow and the open-field regions of two coronal partings) near the sunspot (the black thick contours of umbra and penumbra). CP1 and CP2 refer to the median lines of two open-field regions in panel 8b.

tivity. Baker et al. (2009) argued the relevance of the QSLs location for driving the plasma outflow. Let us exemplify these arguments for the case of the AR 8535. (1) *The occurrence of the outflows observed over or near a unipolar magnetic area.* Indeed, the outflow locates at the side of the sunspot 8535 adjacent to the weak magnetic fields of the same polarity as that of the sunspot. (2) *The outflows are more likely associated with open-field regions.* This is true for the sunspot 8535 since the outflow locates at CP2, which according to PFSS modeling is the region of open field lines. (3) *The outflows persist for several days.* Brosius & Landi (2005) measured Doppler velocities in excess of $5.2{\times}10^4$ m s^{-1} for the outflows at nearly the same location in the AR 8535 on May 9 and May 13.

We suggest that this distinctive region of the plasma outflow is applicable to the tests on its connection to the heliosphere (Slemzin et al. 2013). It can be a primary source of the slow solar wind.

The region where is rooted the CLF with the pronounced separation between the endpoints of the loops is known as an indicator of a QSL (Schrijver, DeRosa & Title 2010).

Warren et al. (2011) commented the tendency of both closed cool loops and plasma outflow, which are associated with the open magnetic structure, to occur in the same area. The authors related this to the specific magnetic topology, but not to the ability of a fan of loops to convey the plasma outflow. The downflows dominate in the bright cool loops, while the outflows occur at higher temperatures, presumably within the open magnetic lines. More recent Doppler velocity measurements of Young, O'Dwyer & Mason (2012) give evidence for the redshifts (plasma downflow) in CLFs under temperatures $T < 8 \times 10^5$ K, while the other group of loops under higher temperatures, $T > (1.3 - -1.6) \times 10^6$ K, shows no perceptible Doppler velocities.

We regard the CLF near the sunspot 8535 as an indicator of the region of plasma outflow but not as a structure able to convey the plasma outflow.

To extend the analogy between the origins of the depressed emission in and outside the sunspot 8535, one needs the strong evidence that there are the extended

in heights ("open") magnetic field lines above the sunspot. Since the near-radial field lines produce the low propagation angles near the time of the CMP, the opacities in o- and x-mode for gyro-resonance microwave radiation and in o-mode for free-free radiation decrease. It is a good reason to suggest the near-radial fields at the heights of microwave radiation.

Nevertheless, we cannot confirm with confidence the extension of the open-field region of the CP2 into the sunspot. It is despite the facts that the dark band of the reduced emission at 5 GHz and 8 GHz and the slightly depressed soft X-ray emission come across the sunspot in line with the open field lines simulated with the PFSS. Some more detailed EUV images are required to discern if the observed dark band of the depressed emission is bordered with the arcades of cool loops. Such arcades are not resolved in the SOHO CDS images.

We suppose that the future model simulations of the microwave radiation of the sunspot-associated source will test the suggestions on the magnetic structure above the sunspot 8535. Then the model results will give the way to the succeeding plasma diagnostics in microwaves.

The conclusions are as follows:

(1) The 8 day-lasting coronal depression seen in the soft X-ray and the SOHO EIT $2.84{\times}10^{-8}$ m images imply the low emission measure for the coronal radiation due to the hot ($T \geq 2 \times 10^6$ K) plasma evacuation in the coronal magnetic structures S1 and S2. The coronal fields simulated with the PFSS model under $R_{\rm SS} = 2.5\ R_\odot$ for S1 and $1.8\ R_\odot$ for S2 appear to be the open-field regions.

(2) There are two indicators of the location of the plasma outflow region within the S2. First, the CLF seen in the TRACE $1.71{\times}10^{-8}$ m images serves as an indicator of the outflow region at the border of the sunspot. Second, the location of the utmost depression of 15 GHz emission in o-mode is taken as one more indicator. Taking into account that the wavelength of the most microwave depression depends on how far distanced is the sunspot from the central solar meridian (Bezrukov et al. 2011), we propose to make use of the microwave observations near the time of the CMP in search for the plasma outflow.

(3) According to the results of the PFSS modeling, the plasma outflow at the border of the sunspot locates in the open-field region. Hence, the two-day observations of blueshifted Doppler velocities performed by Brosius & Landi (2005) have provided a distinctive region of the plasma outflow for the tests on its connection to the heliosphere.

ACKNOWLEDGMENTS. The authors wish to thank Prof. C. E. Alissandrakis for his useful comments on the NoRH data treatment (private communication). This work was partly carried out on the Solar Data analysis System operated by the Astronomy Data Center in cooperation with the Hinode Science Center of the National Astronomical Observatory of Japan.

REFERENCES

Altschuler M. D., Newkirk G. 1969, Solar Physics, 9, 131

Baker D., van Driel-Gesztelyi L., Mandrini C. H., Démoulin P., Murray M. J. 2009, ApJ, 705, 926

Bezrukov D., Ryabov B., Peterova N., Topchilo N. 2011, Latvian Journal of Physics and Technical Sciences, 48(2), 56

Brosius J. W., Landi E. 2005, ApJ, 632, 1196
Brosius J. W., White S. M. 2004, ApJ, 601, 546
Del Zanna G. 2008, A&A, 481, L49
Doschek G. A., Warren H. P., Mariska J. T. et al. 2008, ApJ, 686, 1362
Iwai K., Koshiishi H., Shibasaki K. et al. 2016, ApJ, 816, 91
Loukitcheva M., Solanki S. K., White S. M. 2014, A&A, 561, 133
Mandrini C. H., Baker D., Démoulin P. et al. 2015, ApJ, 809, 73
Moses D., Clette F., Delaboudiniére J.-P. et al. 1997, Solar Physics, 175, 571
Nikulin I. F., Dumin Y. V. 2016, Advances in Space Research, 57, 904
Harrison R. A., Bryans P., Simnett G. M., Lyons M. 2003, A&A, 400, 1071
Ryabov B. I., Gary D. E., Peterova N. G., Shibasaki K., Topchilo N. A. 2015, Solar Physics, 290, 21
Schatten K. H., Wilcox J. M., Ness N. F. 1969, Solar Physics, 6, 442
Schrijver C. J., DeRosa M. L. 2003, Solar Physics, 212, 165; http://www.lmsal.com/∼schryver/Sun/HelioAssim1996_2013.mov
Schrijver C. J., DeRosa M. L., Title A. M. 2010, ApJ, 719, 1083
Scott J. T., Martens C. H., Tarr L. 2013, ApJ, 765, 82
Slemzin V., Harra L., Urnov A. et al. 2013, Solar Physics, 286, 157
Suzuki I., Sakurai T., Ichimoto K. 2006, PASJ, 58, 165
Švestka Z., Solodyna C. V., Howard R., Levin R. H. 1977, Solar Physics, 55, 359
Warren H. P., Ugarte-Urra I., Young P. R., Stenborg G. 2011, ApJ, 727, 58
Young P. R., O'Dwyer B., Mason H. E. 2012, ApJ, 744, 14